Photoinduced electron transfer and geminate recombination in liquids on short time scales: Experiments and theory

Alexei Goun, Ksenija Glusac, and M. D. Fayer[a)]
Department of Chemistry, Stanford University, Stanford, California 94305

(Received 28 November 2005; accepted 19 January 2006; published online 23 February 2006)

The coupled processes of intermolecular photoinduced forward electron transfer and geminate recombination between the (hole) donor (Rhodamine 3B) and (hole) acceptors (*N*,*N*-dimethylaniline) are studied in three molecular liquids: acetonitrile, butyronitrile, and benzonitrile. Two color pump-probe experiments on time scales from ~100 fs to hundreds of picoseconds give information about the depletion of the donor excited state due to forward electron transfer and the survival kinetics of the radicals produced by forward electron transfer. The data are analyzed with a model presented previously that includes distance dependent forward and back electron transfer rates, donor and acceptor diffusion, solvent structure, and the hydrodynamic effect in a mean-field theory of through solvent electron transfer. The forward electron transfer is in the normal regime, and the Marcus equation for the distance dependence of the transfer rate is used. The forward electron transfer data for several concentrations in the three solvents are fitted to the theory with a single adjustable parameter, the electronic coupling matrix element J_f at contact. Within experimental error all concentrations in all three solvents are fitted with the same value of J_f. The geminate recombination (back transfer) is in the inverted region, and semiclassical treatment developed by Jortner [J. Chem. Phys. **64**, 4860 (1976)] is used to describe the distance dependence of the back electron transfer. The data are fitted with the single adjustable parameter J_b. It is found that the value of J_b decreases as the solvent viscosity increases. Possible explanations are discussed.
 [DOI: 10.1063/1.2174009]

I. INTRODUCTION

Liquids are an important medium for electron transfer processes. In spite of the ubiquity of liquids, understanding photoinduced electron transfer between donors and acceptors in liquids remains a challenging problem. Diffusion of donors and acceptors in liquids masks the direct observation of rates of electron transfer reactions, making the elucidation of the distance dependent transfer rates a difficult task. Examination of the back transfer process (geminate recombination) is further complicated because the distribution of radical pair distances is not random but rather determined by the dynamics of the forward transfer process. Measured kinetic curves correspond to the electron transfer kinetics convolved with the transport processes for donor and acceptor. Consequently, to compare theoretical models of the electron transfer with experiments, the appropriate model for the transport in solutions has to be included.

Molecular dynamic and quantum chemistry simulations can be used to create a complete description of the electron transfer process in the solution. However, this approach requires considerable computational resources and so far has not been extended further than tens of picoseconds.[1] Moreover, one is frequently interested in long-term products of chemical reactions, such as the radical escape probability in the electron transfer reaction. In such situations the precision of molecular dynamics simulations is unnecessary, because the only process that happens is the transport of molecules out of the reaction region, and the continuum description provided by the diffusion equation is sufficient. Models based on analytical descriptions of distance dependence of electron transfer and the diffusion equation employ easily accessible parameters of the system studied, such as concentrations, solvent viscosity, and reduction and oxidation potentials of the solutes. Due to the accessibility of these parameters, the continuum-based models can be widely applicable.

For chemical reactions in liquids the relative motion of the reactants and the products needs to be considered. The simplest description of the solvent as an unstructured continuum with freely and independently diffusing particles was found to be inadequate. Attempts to model the kinetics of simplest chemical reactions such as molecular iodine dissociation-recombination encountered a variety of difficulties.[2] More elaborate descriptions of the solvent take into account the correlations in molecular positions as well as the state of their motion. Correlations in particle positions can be introduced through the pair correlation function $g(r)$. Interactions between solvent molecules, responsible for the appearance of solvent structure, also affect the relative motion of the solvent. It was found that the microscopic mechanism of the diffusion in the liquid is cooperative.[3–5] The manifestation of these correlations among molecular pairs is expressed through the introduction of the distance dependent mutual diffusion coefficient $D(r)$.[6,7]

Once the forward electron transfer has occurred, the

[a)]Electronic mail: fayer@stanford.edu

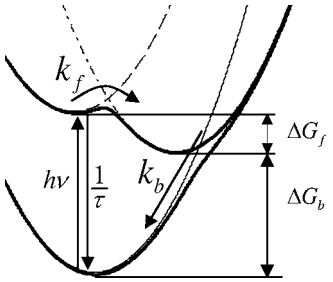

FIG. 1. Schematic of the potential surfaces and dynamic processes. The forward electron transfer is in the normal regime, and the geminate recombination is in the inverted regime.

geminate recombination can take place. Details of the spatial distribution of the radicals involved in the back electron transfer reaction depend sensitively on the parameters of the forward electron transfer. As a consequence, forward electron transfer and geminate recombination kinetics become intrinsically coupled. Previously, the ability of a theoretical model based on the Smoluchowski diffusion equation to correctly describe the process of the photoexcited forward electron transfer in a variety of solvents from subpicosecond to nanosecond time scales has been demonstrated.[8,9] The combined theory of forward electron transfer and geminate recombination was tested once for times >100 ps and demonstrated good agreement with experiment.[10]

In this paper we present experimental data on photoinduced forward electron transfer and geminate recombination in simple polar liquids studied by pump-probe spectroscopy with subpicosecond time resolution. The solvents employed in the study are acetonitrile, butyronitrile, and benzonitrile—a sequence of polar, nonhydrogen bonding liquids of increasing viscosity. The donor-acceptor electron transfer system studied is Rhodamine 3B (R3B)-*N*,*N*-dimethylaniline (DMA). Photoexcited $R3B^+$ ($R3B^*$) accepts an electron, while DMA donates the electron. The $R3B^+$ concentration is much smaller than the DMA concentration, and $R3B^+$ photoexcitation serves as a trigger for the reaction. Consequently, we call R3B the donor (hole donor) and DMA the acceptor (hole acceptor). Once the donor undergoes photoexcitation, the sequence of events depicted in Fig. 1 follows. If there is no acceptor nearby, the donor returns to the ground state through the process of spontaneous emission or nonradiative relaxation. Otherwise the donor-acceptor pair undergoes a charge transfer process with a distance dependent rate constant $k_f(r)$. Once the charge has moved to the acceptor, the competition between charge recombination and radical escape takes place. If the rate of the charge recombination $k_b(r)$ is high enough, most of the radical pairs formed by forward transfer undergo geminate recombination. On the other hand, it is possible for some radical pairs to diffuse apart, resulting in a long-lived population of radicals. Below, the processes of forward electron transfer, geminate recombination, and radical escape will be studied with experiments and theory.

II. THEORY

For any donor-acceptor pair, the rate coefficient of the electron transfer reaction is experiencing fluctuations due to the random motion under the influence of solvent. This makes the rate equation stochastic, which influences the macroscopic behavior of the process. Both molecules diffuse, rarely coming into contact. Due to the short range nature of the electron transfer process, the rate is negligible at most distances, but once molecules come into close proximity, the rate of the forward electron transfer as well as the back electron transfer can be substantial.

The following illustrates the general approach to the statistical description of this problem. Consider a single donor and acceptor pair in the solvent. The kinetic equation that describes the evolution of population of this pair is given by

$$\begin{aligned} dP_{\mathrm{ex}}/dt &= -k_f[\mathbf{r}_{\mathrm{DA}}(t)]P_{\mathrm{ex}}, \\ dP_{\mathrm{CT}}/dt &= k_f[\mathbf{r}_{\mathrm{DA}}(t)]P_{\mathrm{ex}} - k_b[\mathbf{r}_{\mathrm{DA}}(t)]P_{\mathrm{CT}}, \end{aligned} \tag{1}$$

where $k_f(\mathbf{r}_{\mathrm{DA}})$ and $k_b(\mathbf{r}_{\mathrm{DA}})$ are the time dependent forward and back electron transfer rates that both depend on relative position $\mathbf{r}_{\mathrm{DA}}(t)$ of the donor-acceptor pair. P_{ex} is the time dependent probability of finding the donor excited state, and P_{CT} is the time dependent probability of finding the system in the charge transfer state. The random relative position of the donor-acceptor pair satisfies the stochastic Langevein equation, which in simplified form can be written as

$$\xi\frac{\partial \mathbf{r}_{\mathrm{DA}}}{\partial t} = -\nabla U(\mathbf{r}_{\mathrm{DA}}) + \eta(t), \tag{2}$$

where ξ is the friction coefficient of the fluid, $U(\mathbf{r}_{\mathrm{DA}})$ is the potential of the mean force, and $\eta(t)$ is the noise function due to the random forces exerted by the solvent molecules. The friction coefficient and the noise term are related through the fluctuation-dissipation theorem,

$$\langle \eta(t)\,\eta(\tau)\rangle = k_B T \xi \delta(t-\tau), \tag{3}$$

where k_B is the Boltzmann constant, and T is the temperature. Equation (2) was obtained by an analysis of the full dynamics of a two solute-solvent system by Deutch and Oppenheim.[11]

Consequently the averaged behavior of the single donor-acceptor pair can be found in several steps: (1) the set of all possible paths satisfying the Langevein equation [Eq. (2)] is found; (2) along each random trajectory the system of kinetic equations [Eq. (1)] is solved; and (3) solutions are averaged over all possible trajectories. The statistical average over all trajectories of all donor-acceptor pairs is a nontrivial problem that can be solved using the path integral formalism.[12,13]

Lin *et al.* have introduced a mean-field treatment of the forward electron transfer-geminate recombination process in solid solution, where the donor and multiple acceptors are immobile.[14] The starting point for the liquid solution problem is their treatment for solid solution. Rate equations describing a single donor surrounded by a set of n acceptors are

$$\frac{dP_{\mathrm{ex}}}{dt} = -\left[\frac{1}{\tau} + \sum_{i=1}^{n} k_f(r_i)\right] P_{\mathrm{ex}},$$

$$\frac{dP_{\mathrm{CT}}^{i}}{dt} = k_f(r_i) P_{\mathrm{ex}} - k_b(r_i) P_{\mathrm{CT}}^{i}. \tag{4}$$

For every specific configuration, this system of equations can be solved, and the decay of the excited state and the population of the charge transfer state as a function of time are obtained. The quantities of interest are the excited state survival probability $P_{\mathrm{ex}}(t)$ and the charge transfer state (radical) survival probability $P_{\mathrm{CT}}(t)=\Sigma_{i=1}^{n} P_{\mathrm{CT}}^{i}(t)$. Both of these quantities have to be averaged over the static distribution of donor-acceptor distances, with the average performed for P_{CT} depending on the results obtained for P_{ex}.

An ensemble average of the equation for the excited state survival probability was carried out by Inokuti and Hirayama (IH) for solid solution treated as a continuum without excluded volume.[15] Later, IH theory was generalized by Huber to explain the appearance of stretched exponential relaxation in a variety of systems.[16]

To obtain the ensemble averaged equations of Lin *et al.*[14] several assumptions have to be made. The solution of the first equation in Eq. (4) is taken to be independent of the second equation. Using the IH approach the first equation is averaged, and the excited state survival probability $\langle P_{\mathrm{ex}}(t)\rangle$ is obtained. $\langle P_{\mathrm{ex}}(t)\rangle$ is substituted into the second equation of Eqs. (4).

$$\frac{dP_{\mathrm{CT}}^{i}(t)}{dt} = k_f(r_i)\langle P_{\mathrm{ex}}(t)\rangle - k_b(r_i) P_{\mathrm{CT}}^{i}(t). \tag{5}$$

Assuming that all acceptors have statistically identical kinetics, it is possible to write the rate equation for the "typical" acceptor,

$$\frac{d\langle P_{\mathrm{CT}}(t)\rangle}{dt} = k_f(r_i)\langle P_{\mathrm{ex}}(t)\rangle - k_b(r_i)\langle P_{\mathrm{CT}}(t)\rangle, \tag{6}$$

and average over the distribution of acceptors.

Employing these two assumptions, statistical independence of forward-backward transfer and statistical homogeneity of acceptors, the "mean-field" approximation of the electron transfer and geminate recombination in solid solutions is derived.

The solid solution model forms the basis for the extension to liquid solution.[10,17–21] The excited state survival probability is given by

$$P_{\mathrm{ex}}(t) = \exp\left(-\frac{t}{\tau}\right) \times \exp\left(-4\pi C \int_{R_m}^{\infty} [1 - S(t|r_0)] r_0^2 g(r_0) dr_0\right), \tag{7}$$

where τ, C, and R_m denote the donor lifetime, acceptor concentration, and the donor-acceptor contact distance (sum of their radii), respectively. $g(r_0)$ is the radial distribution function that determines the distribution of donor-acceptor distances. $S_{\mathrm{ex}}(t|r_0)$ is the survival probability, that is, the probability that the donor is still in the excited state at time t if it was initially excited at $t=0$ and at the distance r_0 from the acceptor for system with a single donor-acceptor pair. Equation (7) is the result of the statistical averaging over all possible initial donor-acceptor separations.

The excited state survival probability for the single donor-acceptor pair satisfies the following diffusion equation with associated initial and boundary conditions:

$$\frac{\partial}{\partial t} S_{\mathrm{ex}}(t|r_0) = L_{r_0}^{+} S_{\mathrm{ex}}(t|r_0) - k_f(r_0) S_{\mathrm{ex}}(t|r_0),$$

$$S_{\mathrm{ex}}(0|r_0) = 1, \quad \frac{\partial}{\partial r_0} S(t|r_0)\big|_{r_0=R_m} = 0, \quad S_{\mathrm{ex}}(t|\infty) = 1, \tag{8}$$

where the $k_f(r_0)$ is the distance dependent electron transfer rate, and $L_{r_0}^{+}$ is the adjoint of the Smoluchowski operator,

$$L_{r_0}^{+} = \frac{1}{r_0^2} \exp(V(r_0)) \frac{\partial}{\partial r_0}\left(D(r_0) r_0^2 \exp(-V(r_0)) \frac{\partial}{\partial r_0}\right). \tag{9}$$

$V(r_0)$ is the potential. Here it is the potential of the mean force because there are no Coulomb interactions between the donor and acceptor prior to or following electron transfer. Other forms of the potential can be employed.[10] $D(r_0)$ is the distance dependent diffusion coefficient. The potential of the mean force is needed to give the correct description of the equilibrium donor-acceptor distribution, and it is expressed through the radial distribution function $V(r_0)=-\ln(g(r_0))$. The initial condition $S_{\mathrm{ex}}(0|r_0)=1$ implies that after the instantaneous excitation the donor is in a well-defined excited state, independent of the position of the acceptor molecule (no exciplex formation). For very low concentration of donors, relatively low concentration of acceptors, and the nature of the molecules used in the experiments, this is an excellent assumption. However, when the donor is dissolved in a solvent that is the acceptor, the charge transfer process can be influenced by the formation of the exciplexes,[22,23]

The second boundary condition in Eq. (7) indicates that it is impossible for donor and acceptor molecules to approach each other closer than the contact distance $R_m=R_d+R_a$, where R_d and R_a are radii of the donor and acceptor, respectively. The boundary condition on the right indicates that the depletion of the acceptors can be neglected on the time scale of the experiment.

Once the charge is transferred to the acceptor, there are two competing processes: geminate recombination and radical escape (the radical pair becomes separated and geminate recombination does not occur). The probability of finding the system in the charge transferred state is given by

$$P_{\mathrm{CT}}(t) = 4\pi C \int_{R_m}^{\infty} \int_{0}^{t} S_{\mathrm{CT}}(t-t'|r_0) S_{\mathrm{ex}}(t'|r_0) \times P_{\mathrm{ex}}(t') dt' g(r_0) k_f(r_0) r_0^2 dr_0. \tag{10}$$

$S_{\mathrm{CT}}(t|r_0)$ is the survival probability of the charge transferred state for the single donor-acceptor pair problem, that is, the pair is still in the charge transfer at time t if it was created at $t=0$ with the donor-acceptor distance r_0. $S_{\mathrm{CT}}(t|r_0)$ satisfies the equation, analogous to Eq. (8) with the appropriate initial and boundary conditions,

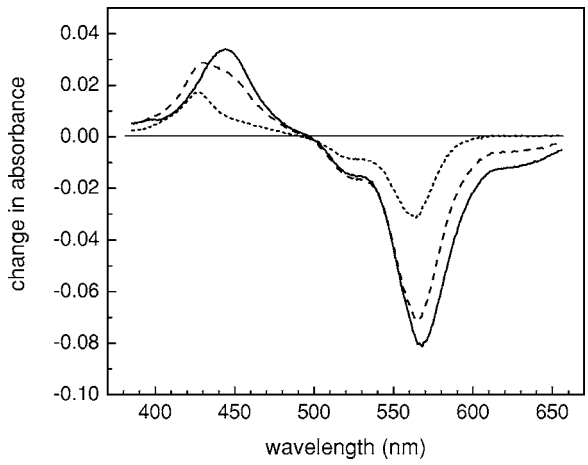

FIG. 2. Transient absorption difference spectra (difference between pump on and pump off) at 8 ps delay between pump and probe. Solid line denotes spectrum for R3B in acetonitrile without DMA acceptors. Dashed line denotes spectrum with DMA acceptors. Dotted line denotes properly normalized difference of spectra without and with acceptors showing the spectrum associated with the production of radicals by forward electron transfer.

$$\frac{\partial}{\partial t}S_{\mathrm{CT}}(t|r_0) = L^{+}_{r_0}S_{\mathrm{CT}}(t|r_0) - k_b(r_0)S_{\mathrm{CT}}(t|r_0),$$

$$S_{\mathrm{CT}}(0|r_0) = 1, \quad \frac{\partial}{\partial r_0}S(t|r_0)|_{r_0=R_m} = 0, \quad S_{\mathrm{CT}}(t|\infty) = 1, \tag{11}$$

where $k_b(r_0)$ is the rate of the electron transfer from acceptor back to the donor.

III. EXPERIMENTAL PROCEDURES

To elucidate the kinetics of the forward and backward charge transfers, we need to measure the kinetics of two species: the photoexcited $R3B^+$, which serves as a donor, and either $R3B^0$ (neutral radical) or DMA^+, the radical products of the forward charge transfer reaction. Because DMA in both its neutral and positively charged states has a small extinction coefficient,[24] the time resolved kinetics of $R3B^+$ and $R3B^0$ were studied.

Time resolved pump-supercontinuum probe spectra of the R3B-DMA solution in acetonitrile are shown on Fig. 2. The solid curve corresponds to the spectrally resolved pump-probe difference spectrum (difference between spectra with and without the pump pulse) of the donor $R3B^*$ without acceptors, and the dashed curve is the difference spectrum with DMA in the solution. Analysis of these two spectra makes it possible to extract kinetic information for the electron transfer system. $R3B^*$ is used to monitor the forward transfer, and $R3B^0$ is used to monitor the back transfer. The important simplifying feature of the spectra is that the wavelength region longer than 620 nm only has a contribution from the stimulated emission of the $R3B^*$. Therefore, this region can be used to monitor its kinetics. Using the $R3B^*$ kinetics, it is possible to eliminate the contribution of $R3B^*$ from the time resolved spectra and obtain the $R3B^0$ kinetics. To obtain the $R3B^0$ kinetics, the pump-probe signal of $R3B^*$ without DMA is scaled to the signal of the R3B-DMA mixture in the wavelength region longer than 620 nm. The scaling factor is used to scale the spectrum of $R3B^*$ without DMA, which is then subtracted from the R3B-DMA mixture signal. The resulting spectrum is the contribution of the charge transferred state ($R3B^0$ radical) to the pump-probe signal, shown as the dotted curve in Fig. 2. To obtain the kinetics at every time separation between pump and probe, one compares the spectrum of $R3B^*$ with DMA against the "ruler," the spectrum of the $R3B^*$ without acceptors. In practice, it is only necessary to measure the data on the two samples at two wavelengths: one in the stimulated emission region (620 nm) and one that has radical absorption.

This procedure can be formalized in the following way. There are four major R3B contributions to pump-probe spectrum: the ground state bleach [(GSB)—depletion of the ground state of $R3B^+$], $R3B^+$ excited state absorption (ESA), stimulated emission (STIM), and absorption of the charge transfer (CT) neutral radical $R3B^0$.

$$S(\lambda,t) = S_{\mathrm{GSB}}(\lambda,t) + S_{\mathrm{ESA}}(\lambda,t) + S_{\mathrm{STIM}}(\lambda,t) + S_{\mathrm{CT}}(\lambda,t). \tag{12}$$

The pump-probe signal at any wavelength λ is determined by the concentrations of the photoactive species and their molar extinction coefficients,

$$S(\lambda,t) = (-\varepsilon_{\mathrm{R3B^+}}(\lambda) + \varepsilon_{\mathrm{ESA}}(\lambda) + \varepsilon_{\mathrm{STIM}}(\lambda)) \times c_{\mathrm{R3B^*}}(t) + (-\varepsilon_{\mathrm{R3B^+}}(\lambda) + \varepsilon_{\mathrm{R3B^0}}(\lambda))c_{\mathrm{R3B^0}}(t). \tag{13}$$

The first negative term in Eq. (13) reflects the contribution to the GSB because $R3B^+$s are in the excited state. The second negative term is the contribution to the GSB because of the generation of CT neutral $R3B^0$ radicals. Wavelengths longer than 620 nm correspond to the stimulated emission of the excited state of $R3B^+$. Consequently, the measurement in this wavelength range allows us to determine the concentration of the photoexcited charge donors.

$$c_{\mathrm{R3B^*}}(t) = \frac{S(620,t)}{\varepsilon_{\mathrm{STIM}}(620)}. \tag{14}$$

Once the concentration of the photoexcited $R3B^+$ is known, the contribution from the excited state $R3B^+$ (ground state bleach and excited-state–excited-state absorption) can be eliminated from the spectrum. The rest is the signal proportional to the charge transfer state $R3B^0$. Because of the scaling procedure there is no need to know the extinction coefficients of various states. It was found that the wavelength that gives the maximum signal for the charge transfer state (radicals) is 565 nm (see Fig. 2, short dash curve), the maximum of the ground state bleach produced by radical generation. Therefore, the time dependent signal of the $R3B^0$ radical state can be found using the following equation:

$$S^{\mathrm{CT}}(565,t) = \left(S^{A}(565,t) - S^{A}(620,t)\frac{S^{0}(565,t)}{S^{0}(620,t)}\right), \tag{15}$$

where S^A is the time resolved pump-probe signal for a sample with acceptors, and S^0 is signal for the sample without acceptors. The wavelengths in nanometer are shown in the parentheses.

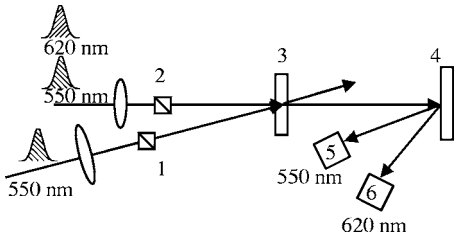

FIG. 3. Schematic of the two color pump-probe experiment. 1 and 2 are polarizers set at the magic angle, 3 is the sample, 4 is the diffraction grating, and 5 and 6 are the photodetectors for the two colors. The two probe colors are collinear passing through the sample and are then separated by the diffraction grating for independent detection.

The experimental difficulty in the measurements lies on the fact that we measure small concentrations of the charge transfer radical, given by Eq. (15), which is obtained as a difference between two rather large signals. Thus, it is necessary to measure each of these signals with very high accuracy, taking care to avoid problems of long-term drifts of pump and probe beams for the samples with and without electron acceptor. To improve the sensitivity of the measurement, single color two color pump-probe measurements were used. The scheme is shown in Fig. 3. The probes (565 and 620 nm) propagate collinearly. The measurements were carried out in a manner to eliminate correlated noise. Instead of additive, noise became multiplicative and did not cause significant degradation of the weak radical signal. Samples with and without acceptors were regularly interchanged under computer control to update the ratio $S^0(565,t)/S^0(620,t)$, which is also sensitive to drifts in pump-probe overlap. Pump-probe experiments were performed at the magic angle to avoid the influence of molecular reorientation.

The output of a Ti:sapphire oscillator/regenerative amplifier was used to pump an optical parametric amplifier (OPA) at 1 kHz repetition rate. The signal output of the OPA at 1.9 μm was summed with a portion of the output of the region, giving a pump pulse at 565 nm. The idler output of the OPA at ~1.25 μm was frequency doubled to give a probe beam at ~620 nm, a wavelength in the range of the stimulated emission of Rhodamine 3B.

IV. RESULTS

The experimental approach described in the previous section provided measurements of both excited state and the charge transferred state (radical) concentrations. The forward electron transfer kinetics and the geminate recombination have common qualitative features in all of the three solvents. We will discuss these using the kinetics in the butyronitrile solvents as an example. The quantitative analysis in all of three solvents will be presented in the next section. Figure 4(a) illustrates the kinetics of the electron transfer process in the butyronitrile for 3 ps, a relatively short time period. The Gaussian curve centered at $t=0$ is the instrument response with a full width half maximum of 200 fs. It is the cross correlation between the 565 nm pump pulse and the 620 nm probe pulse. The cross correlation time limits the resolution of the experiment. Figure 4(b) shows forward electron transfer on an extended time scale. In Figs. 4(a)–4(c), the top

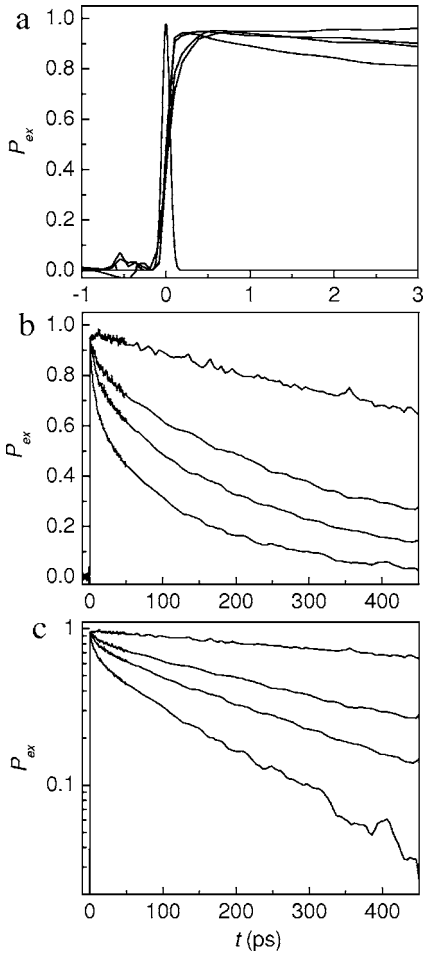

FIG. 4. Examples of the time and concentration dependences of the forward electron transfer. The solvent is butyronitrile. (a) is the data for 3 ps. The Gaussian centered at $t=0$ is the 200 fs instrument response. (b) is the data for 450 ps. (c) is the data on a semilog plot. In all plots the top curve is the decay without acceptors and the other curves (top to bottom) have acceptor concentrations of 0.17M, 0.27M, and 0.48M.

curve shows the excited state lifetime of R3B* in butyronitrile, which is 1.2 ns. The other curves show the kinetics of the forward electron transfer in the presence of acceptor concentrations: 0.17M, 0.27M, 0.48M (top to bottom). The higher the concentration of acceptors, the faster the decay of the excited state due to increased electron transfer. The log scale plot of the excited state kinetics [Fig. 4(c)] shows two regions. The first region, up to ~20 ps, displays nonexponential kinetics, which corresponds to forward electron transfer with one or more acceptors in close proximity to a donor at $t=0$. The electron transfer at short time does not involve significant change in relative position (non-stationary). After ~20 ps, the kinetics of the electron transfer is mainly diffusion controlled. The decays appear exponential, but the decay is dependent on the concentration of acceptors. Previous experiments of this type began at ~50 ps.[9]

The kinetics of the electron transfer state $P_{CT}(t)$ in butyronitrile are shown in Figs. 5(a) and 5(b) on two time scales. The rapid rise of $P_{CT}(t)$ and rapid decay of $P_{ex}(t)$ correspond to the electron transfer in closely spaced donor-acceptor pairs. The charge transfer signal reaches its maximum at ~5 ps. Up to that time, the rate of the forward electron trans-

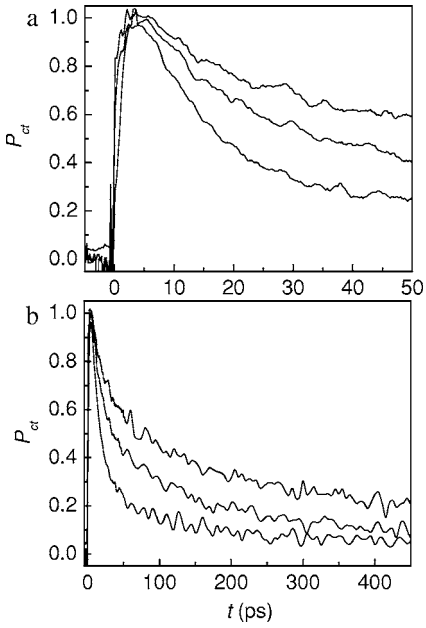

FIG. 5. Examples of the time and concentration dependences of the radical concentration kinetics to 50 ps (a) and 450 ps (b). The solvent is butyronitrile. In (a), the initial rise which occurs as radicals are formed faster than they recombine. The curves (top to bottom) have acceptor concentrations of 0.17M, 0.27M, and 0.48M.

fer exceeds the rate of the geminate recombination. The position of the $P_{CT}(t)$ maximum is independent of the acceptor concentration in the concentration range used in the experiment. After ~5 ps, the geminate recombination rate exceeds the forward electron transfer rate. It can also be seen that the forward electron transfer and the recombination kinetics slow down as time increases. At short times, donors that happen to have acceptors close by rapidly undergo forward electron transfer that produces a radical pair with small separation. For such closely spaced radical pairs, back transfer is rapid and there is little probability that they will diffuse apart prior to geminate recombination. For donors that do not have nearby acceptors, forward transfer will be slower, and more widely separated radical pairs are produced. Geminate recombination will be slower, and there will be increased probability that the pair will diffuse apart before recombination can occur.

Figure 6 displays the data for the forward electron transfer and the radical kinetics in butyronitrile. The experimental curves are offset for clarity (top curves: 0.48M, middle curves: 0.27M, and bottom curves: 0.17M). The amplitudes of each pair of curves have been scaled to match at ~100 ps. There are two time regimes again. At short times the kinetics are dominated by the initial donor-acceptor spatial configurations; the donor-acceptor diffuse flow has not reached steady state. In this regime, the forward electron transfer (upper curve in each pair at short times) dominates the geminate recombination. At longer time, the kinetics of the radicals formed by forward transfer follows rather closely the excited state kinetics. In the three-dimensional space it is possible for the radical pairs to escape recombination, although the exact probability of escape depends on the details of the radical pair interaction. The highest concentration curve

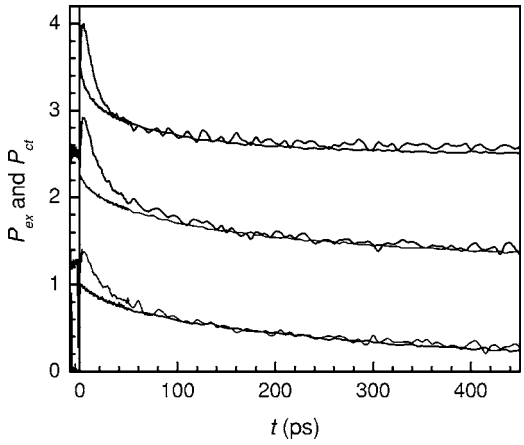

FIG. 6. Data for the forward electron transfer and the radical kinetics in butyronitrile. The experimental curves are offset for clarity (top curves: 0.48M, middle curves: 0.27M, and bottom curves: 0.17M). The amplitudes of each pair of curves have been scaled to match at ~100 ps. The forward electron transfer data are the upper curves in each pair at short times.

(0.48M) displays evidence that there is some escape. From the data, the upper bound on the probability of escape can be placed at 5% of the initial excited donor concentration.

V. COMPARISON TO THEORY

First, the forward electron transfer kinetics will be analyzed quantitatively using Eqs. (7)–(11). To create an accurate quantitative model the electron transfer rate, structural, and transport properties of the solvent have to be known.

The forward electron transfer rate was modeled using the Marcus equation[25–28]

$$k_f(r) = \frac{2\pi}{\hbar\sqrt{4\pi\lambda_S(r)k_BT}} J_f^2 \exp\left(-\frac{(\Delta G_f + \lambda_S(r))}{4\lambda_S(r)k_BT}\right) \times \exp(-\beta_f r) \tag{16}$$

$\lambda_s(r)$ is the solvent reorganization energy,

$$\lambda_s(r) = \frac{e^2}{8\pi\varepsilon_0}\left(\frac{1}{\varepsilon_o} - \frac{1}{\varepsilon_s}\right)\left(\frac{1}{r_d} + \frac{1}{r_a} - \frac{2}{r}\right) + \lambda_i,$$

where ε_o and ε_s are the optical and static dielectric constants, respectively; r_d and r_a are the donor and acceptor radii, respectively; ε_0 is the permittivity of free space; e is the charge of the electron; λ_i=0.10 eV is the inner sphere reorganization energy, Ref. 9. The free energy of the electron transfer reaction ΔG_f was obtained from electrochemical measurements[9] and corrected for the specific dielectric constants of the three solvents. The distance dependence of the forward electron transfer rate is characterized by the parameter β_f, which was fixed at 1 Å for the three solvents, a typical value through solvent electron transfer.[28–32]

The structural and transport properties of the solvent are described by the pair distribution function and the distance dependent diffusion coefficient. The pair distribution function of the solvent was estimated using Percus-Yevick method, in the hard sphere approximation.[33–36] A packing fraction of hard spheres of 45% was used because molecular dynamic simulations predict values between 43% and 48% for dense, room-temperature liquids.[37–39] The solvent contact

TABLE I. Various parameters used in calculations.

Solvent	ε_s	ε_o	η (cP)	T_b (°C)	T_m (°C)	σ (Å)	D_{DA}[a] (Å^2/ns)	D_{rad}[b] (Å^2/ns)
Acetonitrile	36.6	1.8	0.34	82	−42	3.6	440	380
Butyronitrile	20.9	1.9	0.62	118	−110	3.7	240	210
Benzonitrile	25.9	2.3	1.27	191	−11	4.5	120	100

[a]Donor-acceptor ($R3B^*-DMA^0$) diffusion constant.
[b]Radical pair ($R3B-DMA^+$) diffusion constant.

distance was obtained by scaling the solvent contact distance of the acetonitrile using density and molecular weight of the solvent. The packing fraction of the solvent was assumed to be the same. It has been demonstrated that the solute radial distribution function tracks that of the solvent for relatively low solute concentrations.[40] Therefore, the radial distribution function of the solvents was used but adjusted for the donor-acceptor contact distance, which is the sum of the R3B and DMA radii of 4.12 and 2.75 Å, respectively. A detailed discussion of the radial distribution function as used in the determination of donor-acceptor electron transfer in solution has been given.[17,18]

The mutual diffusion coefficient for the donor-acceptor pair was found by scaling the value 438 Å^2/ns found previously by the solvent viscosity.[9] The mutual diffusion coefficients used in the calculations are shown in the Table I. The diffusion coefficient of an ion in a polar liquid is well described by the Stokes-Einstein equation

$$D = \frac{kT}{6\pi R}, \tag{17}$$

where R is the radius of the diffusing ion. Once electron transfer has occurred the donor becomes neutral and its diffusion constant increases. In contrast, the acceptor goes from neutral to charged and its diffusion slows down. To determine the value of the diffusion coefficient after the electron transfer event, the Spernol-Wirtz correction[41,42] for the Stokes-Einstein equation was used.

$$D = \frac{kT}{6\pi R f_{SW}}, \tag{18}$$

where f_{SW} is the Spernol-Wirtz correction factor. To obtain the correction for the diffusion coefficients, melting and boiling temperatures of the solute and solvent have to be known. Solvent melting and boiling temperatures are shown in the Table I. Boiling and melting temperatures for DMA are T_m =2.5 °C and T_b=194 °C.[43] We were unable to find melting and boiling temperatures of R3B, instead we have used parameters of geometrically similar 9-phenylanthracene molecule, T_m=154 °C (Ref. 44) and T_b=417 °C (Ref. 45). For both solute molecules we determined the Spernol-Wirtz correction factors in all of the solvents. These factors are close in magnitude. By our estimates the neutral molecule has the diffusion coefficient approximately 2.8 times larger than its ion. At the same time the mutual diffusion coefficient becomes only 15%–20% smaller after electron transfer. Before the electron transfer, the mutual diffusion is determined primarily by the diffusion coefficient of smaller, neutral DMA. After the electron transfer, the diffusion coefficient of DMA decreases and becomes approximately equal to that of the neutral R3B. Consequently, the change in the value of the mutual diffusion coefficient is not dramatic. The distance dependence of the diffusion coefficient was described by the expression developed by Northrup and Hynes,[46]

$$D(r) = D\left[1 - \frac{1}{2}\exp\left(\frac{r_c - r}{\sigma}\right)\right], \tag{19}$$

where r_c is the donor-acceptor contact distance, and σ is the solvent diameter.

The values of all of the input parameters for the three solvents are given in Table I. With these input parameters, the only unknown parameter is the donor-acceptor electron coupling J_f and, as discussed below, J_b for the back transfer.

Figure 7 shows the forward transfer data and fits to the data for the three solvents [acetonitrile, butyronitrile, and benzonitrile (top panel to bottom panel)] in two forms. The first column shows the data for the three solvents as taken. The top curve in each panel in the first column is the $R3B^*$ lifetime decay in the absence of acceptors. The other three curves in each panel are for the three concentrations (top to bottom) 0.17M, 0.27M, and 0.48M. Each panel also has the result of the simultaneous fits to the three concentrations. The calculated curves are in excellent agreement with the data. The J_f values that produced the fits for the three solvents are J_f=225, 231, and 210 cm^{-1} for acetonitrile, butyronitrile, and benzonitrile, respectively. Within experimental error, these values are the same. The matrix element J_f reflects the magnitude of the electronic interaction between the donor and acceptor at contact. It would be expected to be relatively insensitive to changes in the series of relatively similar solvents. Although the solvents are similar, the diffusion constants, dielectric constants, and radial distribution function vary with solvent. The fact that all of the data could be fitted, the three acceptor concentrations in each of three solvents, with a single adjustable parameter over a substantial range of times, shows that the theoretical description of forward electron transfer works well.

Another way of assessing the efficacy of the theory is shown in the second column of Fig. 7. There is a scaling relationship with concentration for the theoretical curves given in Eq. (20).

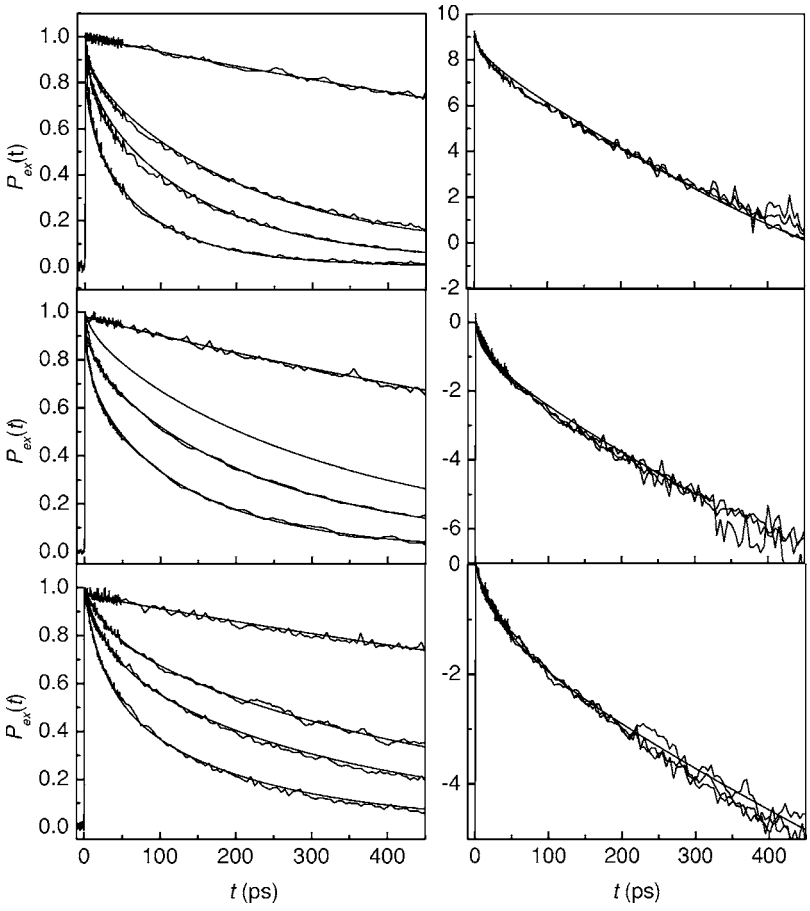

FIG. 7. Forward electron transfer data and fits for the three solvents: acetonitrile, butyronitrile, and benzonitrile (top panel to bottom panel). The top curve in each panel in the first column is the R3B* lifetime decay in the absence of acceptors. The other three curves in each panel are for the three acceptor concentrations: (top to bottom) $0.17M$, $0.27M$, and $0.48M$. All of the forward electron transfer data are fitted with a single adjustable parameter $J_f=220\pm10$ cm^{-1}. The second column shows that the forward electron transfer data obey the scaling relationship, Eq. (17).

$$f(t)=\frac{1}{C}\ln\left[P_{\mathrm{ex}}(t)\exp\left(\frac{t}{\tau}\right)\right]$$
$$=-4\pi\int_{R_m}^{\infty}(1-S_{\mathrm{ex}}(t|r_0))r_0^2g(r_0)dr_0, \quad (20)$$

where $f(t)$ is independent of concentration. If the data are plotted in this manner, the curves for the various concentrations should be superimposable. Second column of Fig. 7 shows the data for each solvent with the three acceptor concentrations plotted as $f(t)$. In addition, the calculated curve, the right hand side of Eq. (20), is also shown. While not absolutely perfect, the data do display the scaling behavior of Eq. (20), and the calculated $f(t)$ describes the scaled data well. The scaling behavior supports the theoretical model for forward transfer.

Geminate recombination is more difficult to deal with both experimentally and theoretically. As discussed above, the radical concentration kinetics must be extracted from the populations of ground state and excited state species. The back transfer kinetics is exceedingly sensitive to the spatial distribution of radical pairs generated by the forward transfer. Therefore, even small errors in the description of the forward transfer can lead to large uncertainties in the description of the geminate recombination. In addition, geminate recombination occurs in the inverted regime; the Marcus form of the transfer rate given in Eq. (16) underestimates the rate of the electron transfer. The tunneling mechanism becomes important: to model the distance dependent back electron transfer rate, a treatment developed by Jortner was employed,[47,48]

$$k_b(r)=\frac{2\pi}{\hbar\sqrt{4\pi\lambda_S(r)k_BT}}J_b^2\sum_{n=0}^{\infty}\frac{e^{-S}S^n}{n!}$$
$$\times\exp\left(-\frac{(\Delta G_b+\lambda_S(r)+nh\nu)}{4\lambda_S(r)k_BT}\right)\exp(-\beta_b r), \quad (21)$$

with $S=\lambda_V/h\nu$. Using Eq. (21) to model the distance dependence of the back transfer adds extra parameters that have unknown values. To avoid introduction of a rather large number of fitting parameters, we have chosen typical values for the mean quantum mode's frequency $\nu=1550$ cm^{-1}, the reorganization energy of the vibrational mode $\lambda_v=0.4$ eV, and $\beta_b=1$ Å, respectively. Therefore, there is again a single adjustable parameter, J_b. A mean frequency of 1550 cm^{-1} corresponds to a typical aromatic stretch, while λ_v values between 0.2 and 0.6 eV are reasonable for aromatic molecules such as Rhodamine 3B and DMA.[31,49]

If the model takes into account all the processes on all the time scales, it should be possible to fit the kinetics of the electron recombination at different DMA concentrations and in different solvents using the same value of the back electron transfer coupling constant. The radical recombination data and the fits to the data are shown for the three solvents in Fig. 8. The top, middle, and bottom panels are for the solvents acetonitrile, butyronitrile, and benzonitrile, respec-

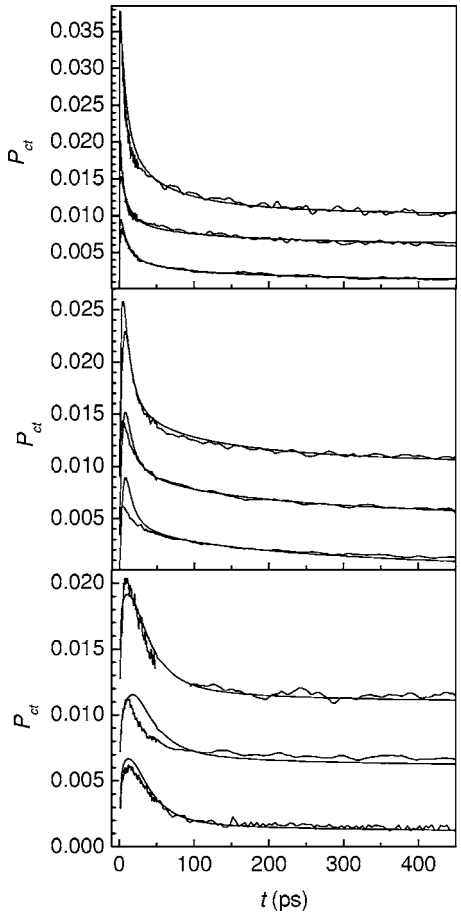

FIG. 8. The radical kinetics data and fits for the three solvents: acetonitrile, butyronitrile, and benzonitrile (top panel to bottom panel). The three curves in each panel are for the three acceptor concentrations: (top to bottom) $0.17M$, $0.27M$, and $0.48M$. All of the forward electron transfer data are fitted with a single adjustable parameter, J_b. Different values of J_b are required for each solvent.

tively. The data for the three concentrations of DMA [$0.17M$, $0.27M$, and $0.48M$ (top to bottom)] have been offset along the vertical axis for clarity. For each solvent, the three curves in each panel (top to bottom) have their zero radical concentrations at 0.01, 0.005, and 0.0 on the vertical axis. The quality of the fits is reasonably good, although it is not nearly as good as those found for the forward electron transfer. The theoretical fits show deviations from the experimental data, particularly at short time. The quality and consistency of the fits with concentration are significantly better for acetonitrile than for the other two solvents.

The fits to the geminate recombination data which yield the matrix elements are $J_b=110$, 53, and 30 cm^{-1} in acetonitrile, butyronitrile, and benzonitrile, respectively. In contrast to the forward transfer data, the back transfer fits are not as good and do not yield the same values of J_b in each solvent. One possible explanation for the change in value of J_b with solvent involves the role of the dependence of the rate of electron transfer on the relative orientation of the radical pair. In both the forward and back transfer theories $R3B^*$, DMA (donor and acceptor), R3B, and DMA^+ (radical pair) are all treated as spheres. In the model, there is no angular dependence to the electronic interaction matrix element. The forward transfer process begins with the donors and acceptors having a random distribution of orientations and a very broad range of separations determined by the radial distribution function. Some of the orientations are undoubtedly more favorable than others, that is, the electronic interaction is a function of angles. However, all angles are present, and while orientational relaxation will take unfavorable orientations into favorable orientations, it will also take favorable orientations in unfavorable ones. In a theoretical study of forward electron transfer, the combined influence of a distribution of distances and orientations without orientational and spatial diffusion was examined.[50] It was found that the time dependence of electron transfer with both angular and distance dependent transfer rates was not significantly different in functional form from the time dependence with a distance dependence only if the distance dependent parameters were changed only slightly.[50] In the absence of an exact knowledge of the distance dependences, the orientational dependence was washed out. Therefore, it is unlikely that it would be possible to observe the influence of orientations on forward electron transfer when the rate of orientational relaxation changes from one solvent to another because of differences in viscosity.

TABLE II. Debye-Stokes-Einstein orientation relaxation times τ_r. R3B and DMA are taken to be spheres with radii of 4.12 and 2.75 Å, respectively.

Solvent	DMA τ_r (ps)	R3B τ_r (ps)
Acetonitrile	70	260
Butyronitrile	130	450
Benzonitrile	260	880

However, the situation for the geminate recombination of radical pairs is quite different from the forward transfer. The distribution of distances and orientations of the radical pairs formed by forward transfer will be determined by the distance and orientation dependence of J_f. The radical pairs will tend to be close together and have the orientations that were *most favorable* for forward transfer. If the angular distribution formed in the forward transfer process is not the most favorable distribution for the geminate recombination, then orientational relaxation could increase the rate of back transfer by taking radical pairs from unfavorable configurations to more favorable configurations. For such a process to be important, orientational relaxation would need to be faster than or at least on the time scale of geminate recombination. Table II lists the orientational relaxation times for DMA and R3B calculated with the Debye-Stokes-Einstein equation

$$\tau_r = \frac{\eta V}{k_B T}, \tag{22}$$

where τ_r is the orientation relaxation time, η is the solvent viscosity, and V is the volume with the molecules approximated as spherical, which is adequate for our purposes. The orientational relaxation times differ substantially for the three solvents. While the orientational sampling cannot be ruled out, the orientational relaxation times are relatively slow. The orientational relaxation of R3B in all three solvents is too slow to play a role. The fastest orientational relaxation time is 73 ps for DMA in acetonitrile. In all three

TABLE III. Estimation of the longitudinal relaxation times τ_L of the solvents.

Solvent	τ_L (ps)
Acetonitrile	8
Butyronitrile	29
Benzonitrile	103

solvents, >50% of the geminate recombination has occurred in <50 ps. The range of angles sampled at relatively short times in the three solvents decreases as for the solvent viscosity increases. This is the same trend as for the J_b's. Therefore, it is possible that the decrease in J_b's with increasing solvent viscosity is the result of a time dependent angular dependence of the transfer rate that has the effect of decreasing the angle averaged J_b as the rate of orientational relaxation slows.

Another time dependent effect that is not taken into account explicitly in the theory is the longitudinal relaxation of the solvent that occurs following forward electron transfer. Prior to electron transfer, $R3B^+$ is positively charged and DMA is neutral. Following electron transfer, R3B is a neutral radical and DMA^+ is a positive radical. The longitudinal relaxation time τ_L of the solvent, that is, the time for the solvent to fully solvate the change in the charge distribution, can be calculated approximately using[51]

$$\tau_L = \frac{\varepsilon_o}{\varepsilon_s}\tau_D, \tag{23}$$

where ε_o and ε_s are the optical and static dielectric constants, respectively, and τ_D is given in Eq. (22). In Eq. (21), ΔG_b is the equilibrium value obtained from the optical transition energy and ΔG_f, which was determined electrochemically. Following the forward transfer, it will take $\sim\tau_L$ to obtain the equilibrium value. At shorter times, ΔG_b will be larger than the equilibrium value, and systems will be farther into the inverted regime, which should reduce the rate of geminate recombination. Table III gives the estimates of τ_L for the three solvents and the parameters used to calculate them. The viscosities are in Table I. The τ_L's fall in a range that could produce a significant solvent dependence that would be manifested in the fitting as differences in J_b's. In acetonitrile, most of the geminate recombination is on the time scale of or significantly slower than τ_L. Butyronitrile is intermediate, and in benzonitrile, most of the geminate recombination occurs at times less than τ_L. In contrast to the orientational relaxation times, the longitudinal relaxation times span the range of times that could be responsible for the trend observed in the J_b's. It is important to note that there is also a very fast (hundreds of femtoseconds) inertial component to the solvation following electron transfer. This component would be expected to be larger and faster in acetonitrile[52] and become progressively smaller and slower as the solvent viscosity increases. Therefore, in acetonitrile, the geminate recombination will essentially occur with the equilibrium value of ΔG_b. This may explain why the quality of the fits for the data taken in acetonitrile is much better than for the other two solvents where solvation is occurring on the time scale of the geminate recombination. While consideration of the differences in solvation is suggestive, it is certainly not conclusive and other solvent dependent properties, such as the mean quantum mode's frequency in Eq. (20), could change with solvent.

VI. CONCLUDING REMARKS

In this paper we have addressed the coupled problems of forward electron transfer and geminate recombination in liquid solutions. Dilute $R3B^+$ was photoexcited and acted as the hole donor to DMA (hole acceptor) in several concentrations in three solvents. Using transient absorption to observe the simulated emission and ground state bleach of $R3B^+$, it was possible to follow both the forward electron transfer to produce radicals and the recombination of the radicals. The forward transfer process is in the normal regime of electron transfer. The radicals formed by electron transfer display a long-lived component, and analysis shows that a few percent of the radicals escape geminate recombination in spite of the fact that forward electron transfer has a very limited spatial extent and occurs mostly between donors and acceptors that are in close proximity.

A statistical mechanics theory was applied to the data to determine if the dynamics could be described with the model that had previously been tested on longer time scales (>50 ps) for forward electron transfer in a variety of solvents[9] and only once for geminate recombination in a single solvent.[10] The theory includes[10] the distance dependence of the transfer rate, diffusion of the donors and acceptors, the radial distribution function that describes the concentration of acceptors near a donor, and the hydrodynamic effect (donor-acceptor separation dependence of the diffusion constant). In fitting the forward electron transfer data a single adjustable parameter was used, J_f, the electronic coupling matrix element at donor-acceptor contact. It was possible to fit three concentrations in each of three solvents with a single value of J_f (220 ± 10 cm^{-1}) within experimental uncertainty. The agreement between the calculated curves from the fits and the data was very good.

The theoretical description of the geminate recombination is more complex with more uncertainties. The geminate recombination dynamics are exceedingly sensitive to the spatial distribution of radical pairs formed by the forward transfer process. Even a small error in the description of the forward transfer can lead to substantial errors in the geminate recombination calculation. The agreement between theory and data was reasonable but not excellent. The shapes of the curves were approximately correct, particularly for the data taken with acetonitrile as the solvent. For each solvent, it was possible to fit the data from samples with different acceptor concentrations with a single adjustable parameter, J_b, the electronic coupling matrix element at contact between the radicals. However, each solvent gave a different value of J_b, with J_b decreasing as the solvent viscosity increased. Possible explanations for the differences in J_b with solvent were discussed.

In previous experiments that examined forward transfer in liquids[9] and geminate recombination[10] the time scale of

the measurements, >50 ps, resulted in diffusion controlling most of the dynamics, although it was still necessary to use a distance dependent transfer rate, diffusion, the radial distribution function, and the hydrodynamic effect to describe the data. In the experiments presented here, measurements examined the dynamics from ~200 fs to hundreds of picoseconds. In the very short time regime, the forward electron transfer is dominated by the essentially static distribution of donors and acceptors that exist at the time of the excitation pulse. The forward transfer that occurs at short times is to nearby acceptors, producing closely spaced radical pair. The closely spaced radical pairs undergo rapid geminate recombination. As can be seen in Figs. 5, 6, and 8, a great deal of the geminate recombination occurs at times <50 ps. The very good agreement between theory and experiments for the forward transfer and the reasonable agreement for geminate recombination demonstrate that the theory can describe electron transfer kinetics for both very closely spaced initially static donor-acceptor distributions and the longer time scale diffusion controlled distance distribution.

ACKNOWLEDGMENTS

One of the authors (A.G.) thanks the W. M. Keck Foundation for support, and another author (K.G.) thanks the American Chemical Society, Petroleum Research Fund for their support. This research was supported by the Department of Energy (DE-FG03-84ER13251).

[1] P. O. J. Scherer and M. Tachiya, J. Chem. Phys. **118**, 4149 (2003).
[2] R. M. Noyes, Prog. React. Kinet. **1**, 129 (1961).
[3] P. L. Fehder, C. A. Emeis, and R. P. Futrelle, J. Chem. Phys. **54**, 4921 (1971).
[4] U. Balucani and R. Vallauri, Physica A **102**, 70 (1980).
[5] S. W. Haan, Bull. Am. Phys. Soc. **24**, 393 (1979).
[6] R. Zwanzig, Adv. Chem. Phys. **15**, 325 (1969).
[7] J. M. Deutch and B. Felderho, J. Chem. Phys. **59**, 1669 (1973).
[8] V. O. Saik, A. A. Goun, J. Nanda, K. Shirota, H. L. Tavernier, and M. D. Fayer, J. Phys. Chem. A **108**, 6696 (2004).
[9] H. L. Tavernier, M. M. Kalashnikov, and M. D. Fayer, J. Chem. Phys. **113**, 10191 (2000).
[10] K. Weidemaier, H. L. Tavernier, S. F. Swallen, and M. D. Fayer, J. Phys. Chem. A **101**, 1887 (1997).
[11] J. M. Deutch and I. Oppenheim, J. Chem. Phys. **54**, 3547 (1971).
[12] L. Onsager and S. Machlup, Phys. Rev. **91**, 1505 (1953).
[13] M. O. Vlad, R. Metzler, T. F. Nonnenmacher, and M. C. Mackey, J. Math. Phys. **37**, 2279 (1996).
[14] Y. Lin, R. C. Dorfman, and M. D. Fayer, J. Chem. Phys. **90**, 159 (1989).
[15] M. Inokuti and F. Hirayama, J. Chem. Phys. **43**, 1978 (1965).
[16] D. L. Huber, Phys. Rev. B **31**, 6070 (1985).
[17] S. F. Swallen, K. Weidemaier, and M. D. Fayer, J. Chem. Phys. **104**, 2976 (1996).
[18] S. F. Swallen, K. Weidemaier, H. L. Tavernier, and M. D. Fayer, J. Phys. Chem. **100**, 8106 (1996).
[19] R. C. Dorfman, Y. Lin, and M. D. Fayer, J. Phys. Chem. **94**, 8007 (1990).
[20] A. I. Burshtein, Chem. Phys. Lett. **194**, 247 (1992).
[21] R. C. Dorfman and M. D. Fayer, J. Chem. Phys. **96**, 7410 (1992).
[22] S. Iwai, S. Murata, R. Katoh, M. Tachiya, K. Kikuchi, and Y. Takahashi, J. Chem. Phys. **112**, 7111 (2000).
[23] S. Iwai, S. Murata, and M. Tachiya, J. Chem. Phys. **114**, 1312 (2001).
[24] V. O. Saik, A. A. Goun, and M. D. Fayer, J. Chem. Phys. **120**, 9601 (2004).
[25] R. A. Marcus, J. Chem. Phys. **24**, 966 (1956).
[26] R. A. Marcus, J. Chem. Phys. **24**, 979 (1956).
[27] R. A. Marcus, Annu. Rev. Phys. Chem. **15**, 155 (1964).
[28] R. A. Marcus and N. Sutin, Biochim. Biophys. Acta **811**, 265 (1985).
[29] H. B. Gray and J. R. Winkler, Annu. Rev. Biochem. **65**, 537 (1996).
[30] G. L. Closs and J. R. Miller, Science **240**, 440 (1988).
[31] J. R. Miller, J. V. Beitz, and R. K. Huddleston, J. Am. Chem. Soc. **106**, 5057 (1984).
[32] T. Guarr and G. McLendon, Coord. Chem. Rev. **68**, 1 (1985).
[33] J. K. Percus, Phys. Rev. Lett. **8**, 462 (1962).
[34] J. K. Percus and G. J. Yevick, Phys. Rev. **110**, 1 (1958).
[35] M. S. Wertheim, Phys. Rev. Lett. **10**, 321 (1963).
[36] E. Thiele, J. Chem. Phys. **39**, 474 (1963).
[37] J. P. Hansen and I. R. McDonald, *Theory of Simple Liquids* (Academic, London, 1976).
[38] L. Verlet and J. J. Weis, Phys. Rev. A **5**, 939 (1972).
[39] D. A. McQuarrie, *Statistical Mechanics* (Harper & Row, New York, 1976).
[40] G. J. Throop and R. J. Bearman, J. Chem. Phys. **44**, 1423 (1966).
[41] A. Spernol and K. Wirtz, Zeitschrift.Fur Naturforschung. Section A. Journal of Physical Sciences **8**, 522 (1953).
[42] H. S. Sandhu, J. Magn. Reson. (1969-1992) **17**, 34 (1975).
[43] J. A. Riddick and W. B. Bunger, *Organic Solvents: Physical Properties and Methods of Purification*, 4th ed. (Wiley-Interscience, New York, 1986).
[44] P. G. Farrell, F. Shahidi, F. Casellato, C. Vecchi, and A. Girelli, Thermochim. Acta **33**, 275 (1979).
[45] R. C. Weast and J. G. Grasselli, *CRC Handbook of Data on Organic Compounds*, 2nd ed. (CRC, Boca Raton, Florida, 1989).
[46] S. H. Northrup and J. T. Hynes, J. Chem. Phys. **71**, 871 (1979).
[47] J. Jortner, J. Chem. Phys. **64**, 4860 (1976).
[48] J. Jortner and M. Bixon, J. Chem. Phys. **88**, 167 (1988).
[49] T. Asahi, M. Ohkohchi, R. Matsusaka, N. Mataga, R. P. Zhang, A. Osuka, and K. Maruyama, J. Am. Chem. Soc. **115**, 5665 (1993).
[50] R. P. Domingue and M. D. Fayer, J. Chem. Phys. **83**, 2242 (1985).
[51] P. Debye, *Polar Molecules* (Dover, New York, 1929).
[52] J. Ruthmann, S. A. Kovalenko, N. P. Ernsting, and D. Ouw, J. Chem. Phys. **109**, 5466 (1998).